

# Focusing waves in an unknown medium without wave field decomposition

Mert S. R. Kiraz<sup>†</sup>, Roel Snieder<sup>†</sup> & Kees Wapenaar<sup>\*</sup>

<sup>†</sup>*Center for Wave Phenomena, Colorado School of Mines, Golden CO 80401, USA*  
email kiraz@mines.edu

<sup>\*</sup>*Department of Geoscience and Engineering, Delft University of Technology, P.O. Box 5048, Delft, GA 2600, The Netherlands*

## ABSTRACT

The Gel'fand-Levitan equation, the Gopinath-Sondhi equation, and the Marchenko equation are developed for 1D inverse scattering problems. Recently, a version of the Marchenko equation based on wave field decomposition has been introduced for focusing waves in multi dimensions. However, this wave field decomposition is a limitation when waves propagate horizontally at the focusing level. We derive the Marchenko equation for focusing without wave field decomposition. By iteratively solving the Marchenko equation, we retrieve the Green's function for an arbitrary location in the medium from the scattered waves recorded on a closed receiver array and an estimate of the direct-wave without using wave field decomposition.

## 1 INTRODUCTION

Inverse scattering (Chadan and Sabatier, 1989; Colton and Kress, 1998; Gladwell, 1993) uses scattered waves to determine the scattering properties of a medium. Burridge (1980) shows that the Gel'fand-Levitan equation and the Gopinath-Sondhi equation have the same structure as the Marchenko equation, and shows that the Marchenko equation can be used for medium reconstruction (Burridge, 1980; Newton, 1980a). The solution of the one-dimensional (1D) Marchenko equation is an exact integral equation to make the connection between the scattered data and the scatterer potential. Rose (2001, 2002) defines focusing as finding an incident wave that becomes a delta function at a prescribed focus location and time inside the medium. He shows that this incident wave follows from the scattered data and uses the Marchenko equation for 1D inverse scattering problems. Brogini and Snieder (2012) utilize Rose's approach and introduce a scheme in 1D to retrieve the Green's function containing single-scattered and multiply-scattered waves of the inhomogeneous medium. Wapenaar et al. (2012) show the virtual source creation in two dimensions using the recorded data but the proposed method excludes horizontally propagating energy at the virtual source level. Wapenaar et al. (2013, 2014) derive the three-dimensional Marchenko equation for wave field focusing and, therefore, for the Green's function retrieval; however, their solution requires up/down decomposition of the wave field, which also excludes horizontally propagating energy at the focusing level. This is a limitation when the medium has steeply dipping structures because the horizontally scattered waves and refracted waves cannot be fully represented with the up/down decomposition. Recently, there have been several studies to address the limitation of the Marchenko method due to the up/down separation of the Marchenko equation. Kiraz et al. (2020) show wave field focusing for an arbitrary point inside an unknown highly scattering inhomogeneous medium using the data acquired on a closed boundary. Diekmann and Vasconcelos (2021) and Wapenaar et al. (2021) present alternative approaches to Green's function retrieval without up/down decomposition each with their own pros and cons.

The Marchenko schemes proposed in 1D provide an exact solution for focusing, and for Green's function retrieval in the medium. Green's function retrieval is of importance for imaging applications in many fields. The ability to focus waves opens up applications ranging from scattering kidney stones to performing imaging, monitoring in seismology, and non-destructive testing.

In this paper, we propose a two-dimensional (2D) Marchenko equation for focusing waves in a highly scattering inhomogeneous medium. We show that by iteratively solving the Marchenko equation, the Green's function for an arbitrary point in a strongly scattering inhomogeneous medium can be retrieved without wave field decomposition at the focal point. As opposed to the current Marchenko algorithms that use single-sided acquisition methods, we include waves propagating in all directions at the focal point using the contributions from a closed array. Our scheme is an extension of the 1D Marchenko algorithms proposed by Newton (1980a), Rose (2001, 2002), and Brogini and Snieder (2012) into 2D.

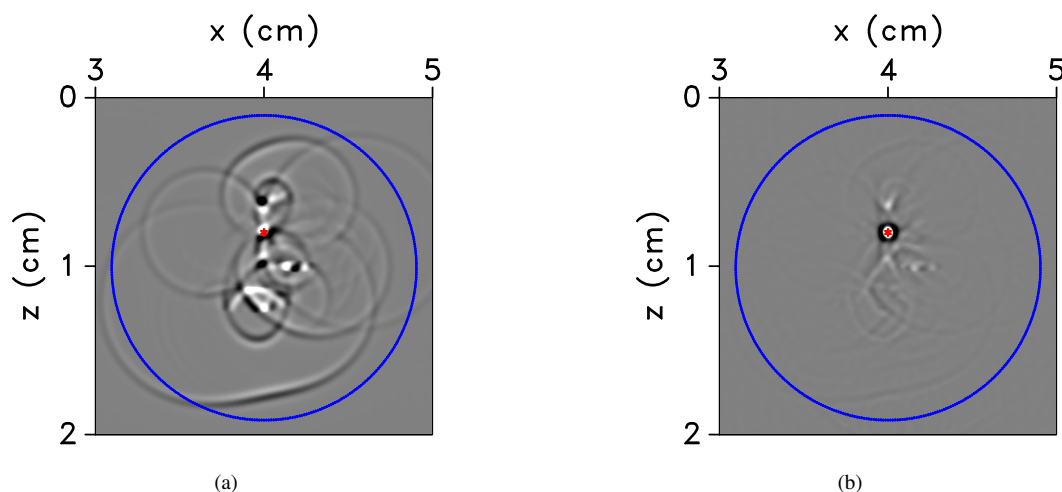


**Figure 1.** (a) Snapshot at  $t = 0$  of the time-derivative of the time-reversed modeled direct-wave injection. (b) Snapshot at  $t = 0$  of the time-derivative of the time-reversed retrieved homogeneous Green's function injection obtained from our iterative Marchenko algorithm. The red asterisk denotes the focal point  $\mathbf{x}_s$  and the blue line represents the transducer locations.

## 2 THEORY

Consider the acoustic wave equation

$$\rho \nabla \cdot \left( \frac{1}{\rho} \nabla p \right) + \frac{\omega^2}{c^2} p = f, \quad (1)$$

where  $\rho$  is density,  $\omega$  is the angular frequency,  $f$  is the source term,  $p$  is pressure, and  $c$  is the velocity. We use the acoustic wave equation for a constant velocity and variable density in the numerical examples in this paper.

We define the Green's function,  $G(\mathbf{x}, \mathbf{x}_s, t)$ , as the solution to the wave equation  $LG = \delta(\mathbf{x} - \mathbf{x}_s)\delta(t)$ , with the differential operator  $L = \rho \nabla \cdot (\rho^{-1} \nabla) - c^{-2} \partial^2 / \partial t^2$ . Here,  $\mathbf{x}_s$  is the source location and the Green's function is the response to a source at  $\mathbf{x}_s$  recorded at the receiver location  $\mathbf{x}$ . We use the following convention for the Fourier transform:  $f(t) = \frac{1}{2\pi} \int F(\omega) \exp(-i\omega t) d\omega$ , where  $i$  is the imaginary unit. In the frequency domain  $G(\mathbf{x}, \mathbf{x}_s, \omega)$  satisfies  $LG = \delta(\mathbf{x} - \mathbf{x}_s)$ , with the differential operator  $L = \rho \nabla \cdot (\rho^{-1} \nabla) + \omega^2 / c^2$ .

We describe an iterative solution to focus a wave field in the medium to a pre-defined location at  $t = 0$  when injected into the medium. Our solution requires the direct-wave information modeled in the homogeneous medium (when  $\rho$  and  $c$  are constant) for a source at the focusing point  $\mathbf{x}_s$ . This is the known Green's function  $G_0(\mathbf{x}, \mathbf{x}_s, t)$  in a homogeneous medium. Sending this direct-wave back into the inhomogeneous medium from a circular receiver array with the radius  $R$  in a time-reversed order creates a focus at the focal point at  $t = 0$ ; however, in addition to the focal spot, other waves are present around the focusing point, and Fig. 1(a) shows the snapshot at  $t = 0$  of the time-reversed direct-wave injection into the heterogeneous medium shown in Fig. 2 (about which the details will be provided in the following section). This shows that emitting the time-reversed direct-wave into an inhomogeneous medium does not restrict the focused field to the focusing point, and our goal is to remove the waves at other locations than the focusing point in Fig. 1(a). Fig. 1(b) shows the snapshot at  $t = 0$  of the wave field injection obtained by the iterative algorithm we propose. As shown in Fig. 1(b), our algorithm creates a wave field that focuses to the pre-defined focal point, which acts as a virtual source, and suppresses other waves at  $t = 0$ . We obtain our focusing wave field by only using the direct-wave information modeled in the homogeneous medium (when  $\rho$  and  $c$  are constant) and the recorded scattering response. Unlike the conventional Marchenko methods, our method does not require the decomposition of the Marchenko equation to achieve focusing. In the following section, we discuss the iterative Marchenko equation we propose for wave field focusing and show how to obtain better focuses in the medium than one can achieve with the direct waves only.

### 2.1 Iterative Scheme and the Marchenko equation

We define the ingoing wave field,  $U^{in}(\hat{\mathbf{n}}', t)$ , and outgoing wave field,  $U^{out}(\hat{\mathbf{n}}, t)$ , where  $\hat{\mathbf{n}}'$  and  $\hat{\mathbf{n}}$  denote the locations on the circle with radius  $R$ ; they are related via the scattering response  $A(\hat{\mathbf{n}}, \hat{\mathbf{n}}', t)$  of the inhomogeneous medium. Following Rose (2001,

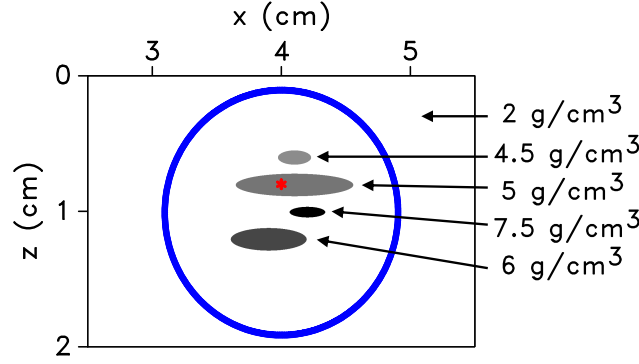


**Figure 2.** Geometry of the 2D model. Sources and receivers (400 each) are located on the blue circle, and the red asterisk shows the virtual source location  $\mathbf{x}_s$ . The elliptical scatterers have contrasting densities which are given on the right hand side.

2002); Broggini and Snieder (2012); Wapenaar et al. (2013, 2014), we design a wave field that becomes a delta function at the focus location with an iterative scheme that relates the ingoing wave  $U_k^{in}$  to the outgoing wave  $U_k^{out}$  at iteration  $k$  as

$$U_k^{out}(\hat{\mathbf{n}}, t) = \oint A(\hat{\mathbf{n}}, \hat{\mathbf{n}}', t - \tau) U_k^{in}(\hat{\mathbf{n}}', \tau) d\tau dn' . \quad (2)$$

The ingoing and outgoing waves and the scattering operator are defined on a circle with radius  $R$ , but for brevity, we omit the parameter dependence on  $R$  in Eq. (2).

The iterative scheme starts with injecting a delta function into the medium and the ingoing wave field for the first iteration gives

$$U_0^{in}(\hat{\mathbf{n}}', \tau) = \delta(\tau + t_d(\hat{\mathbf{n}}')) , \quad (3)$$

where  $t_d(\hat{\mathbf{n}}')$  is the arrival time of the direct waves that propagates from the focusing point to the point  $\hat{\mathbf{n}}'$  on the circle.

Following Broggini and Snieder (2012), the purpose of the iterative scheme is to reconstruct a wave field that after interacting with the heterogeneities in the medium collapses onto a delta function at the focusing point at  $t = 0$ . We create a symmetric field in time for  $-t_d(\hat{\mathbf{n}}') < t < t_d(\hat{\mathbf{n}}')$ . We later show that the symmetry in time leads to focusing. To achieve the symmetry for the iterative scheme, we define the ingoing wave field as

$$U_k^{in}(\hat{\mathbf{n}}', \tau) = U_0^{in}(\hat{\mathbf{n}}', \tau) - \Theta(\hat{\mathbf{n}}', \tau) U_{k-1}^{out}(\hat{\mathbf{n}}, -\tau) , \quad (4)$$

where  $\Theta(\hat{\mathbf{n}}', \tau)$  is a window function and defined as  $\Theta(\hat{\mathbf{n}}', \tau) = 1$  when  $-t_d(\hat{\mathbf{n}}') < \tau < t_d(\hat{\mathbf{n}}')$ , and otherwise  $\Theta(\hat{\mathbf{n}}', \tau) = 0$ .

When the iterative scheme converges (hence when  $U_k^{out} = U_{k-1}^{out}$ ), the iteration number can be dropped. Inserting Eq. (4) into Eq. (2) then gives

$$U^{out}(\hat{\mathbf{n}}, t) = \oint \int A(\hat{\mathbf{n}}, \hat{\mathbf{n}}', t - \tau) U_0^{in}(\hat{\mathbf{n}}', \tau) d\tau dn' - \oint \int_{-t_d}^{t_d} A(\hat{\mathbf{n}}, \hat{\mathbf{n}}', t - \tau) U^{out}(\hat{\mathbf{n}}', -\tau) d\tau dn' , \quad (5)$$

with  $t_d^\epsilon = t_d - \epsilon$  where we introduce  $\epsilon$  as a small positive constant to exclude the direct-wave at  $t_d$ . If we define  $K = -U^{out}$ , and substitute this into Eq. (5) using Eq. (3), we obtain

$$K(\hat{\mathbf{n}}, t) + \oint A(\hat{\mathbf{n}}, \hat{\mathbf{n}}', t + t_d(\hat{\mathbf{n}}')) dn' + \oint \int_{-t_d}^{t_d} A(\hat{\mathbf{n}}, \hat{\mathbf{n}}', t - \tau) K(\hat{\mathbf{n}}', -\tau) d\tau dn' = 0 . \quad (6)$$

Burridge (1980) shows that the 1D Marchenko equation, Gel'fand-Levitan equation, and the Gopinath-Sondhi equations of inverse scattering can be written in symbolic notation as  $K + R + \int_W RK = 0$  where  $\int_W$  shows the time interval,  $R$  is the recorded data, and  $K$  is the function we solve for. Eq. (6) has the same structure as the equations derived by Burridge (1980) and, therefore, gives a 2D Marchenko equation without using up/down decomposition. Eq. (6) also has a similar relation with the equations derived by Newton (1980b, 1981, 1982) using the scattering data in multi-dimensional media.

### 3 NUMERICAL EXAMPLE AND GREEN'S FUNCTION RETRIEVAL

We illustrate our method with a 2D numerical example. Fig. 2 shows the source and receiver geometry of a 2D acoustic medium. The red asterisk in Fig. 2 denotes the virtual source location and the blue line represents a circle on which 400 equidistant sources

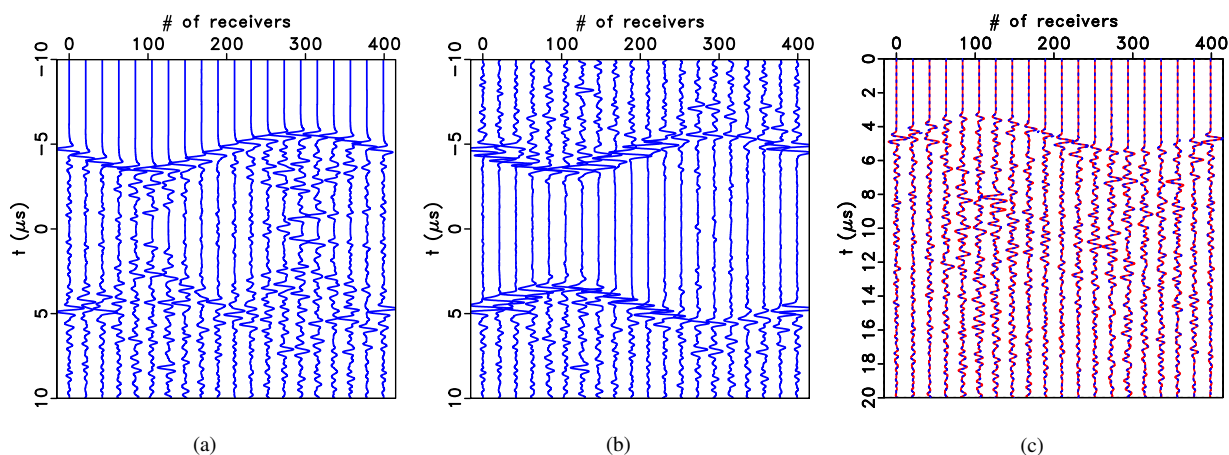


**Figure 3.** (a)  $U_{total}(\hat{\mathbf{n}}', t)$  for the 7th iteration. (b)  $U_{total}(\hat{\mathbf{n}}', t) - U_{total}(\hat{\mathbf{n}}', -t)$ . (c) Comparison of the calculated (red line) and the retrieved (blue line) Green's functions. The traces have been multiplied by  $\exp(2t)$  to emphasize the scattered waves.

and receivers are placed. The virtual source location,  $\mathbf{x}_s = (x, z)$ , is at  $x = 4$  cm and  $z = 0.8$  cm. The medium has a constant background velocity and density,  $c_0 = 2$  km/s and  $\rho_0 = 2$  g/cm<sup>3</sup>, respectively. Fig. 2 also shows four different elliptical-shaped scatterers located in the medium with densities  $\rho_1 = 4.5$  g/cm<sup>3</sup>,  $\rho_2 = 5$  g/cm<sup>3</sup>,  $\rho_3 = 7.5$  g/cm<sup>3</sup>,  $\rho_4 = 6$  g/cm<sup>3</sup>, respectively. We use finite-difference modeling with absorbing boundaries and the source wavelet is a Ricker wavelet (Ricker, 1953) with a central frequency of 2 MHz. A challenge of the used geometry is that the focusing point is located inside one of the scatterers, which has a reflection coefficient of about 40% at the boundaries. As a result, the source generates strong reverberations within the scatterer.

The ingoing wave field in the finite-difference modeling can be implemented by either changing the finite-difference stencil at the circular array, or by using the equivalent sources  $f$  (in equation form) in the acoustic wave equation (1) to produce the desired ingoing wave field. We use the equivalent sources in the acoustic wave equation (1) for the finite-difference implementation where the equivalent sources are given by the normal derivative of the ingoing wave field. To solve the Marchenko equation iteratively, we start with  $U_0^{in}(\hat{\mathbf{n}}', t) = U_d(\hat{\mathbf{n}}', -t)$  where  $U_d$  is the time-reversed direct-wave in the homogeneous background medium. We send the ingoing wave  $U_0^{in}$  from the receiver array into the medium and use the outgoing wave recorded at the array in Eq. (4) to determine the ingoing wave for the next iteration. We use seven iterations to get close to convergence but more iterations might be needed for more complicated media where velocity and density are varying.

We next inject the wave field obtained by the iterative solution on the boundary. Fig. 3(a) shows the total wave field,  $U_{total}(\hat{\mathbf{n}}', t) = U^{in}(\hat{\mathbf{n}}', t) + U^{out}(\hat{\mathbf{n}}', t)$ , recorded on the boundary for the 7th iteration, which consists of the superposition of the ingoing and outgoing wave field. The wave field in Fig. 3(a) is symmetric in time for  $-t_d(\hat{\mathbf{n}}') < t < t_d(\hat{\mathbf{n}}')$  (approximately between  $-5$   $\mu$ s and  $5$   $\mu$ s). If we take the difference between the total wave field in Fig. 3(a) and its time-reversed version, i.e.,  $U_{total}(\hat{\mathbf{n}}', t) - U_{total}(\hat{\mathbf{n}}', -t)$ , all events in the interval  $-t_d(\hat{\mathbf{n}}') < t < t_d(\hat{\mathbf{n}}')$  vanish as shown in Fig. 3(b). A small amount of energy remains in Fig. 3(b) for  $-t_d(\hat{\mathbf{n}}') < t < t_d(\hat{\mathbf{n}}')$ , this is due to numerical inaccuracies in our solution of the Marchenko equation. Since  $U_{total}(\hat{\mathbf{n}}', t) - U_{total}(\hat{\mathbf{n}}', -t)$  is anti-symmetric in time, it vanishes for  $t = 0$ , also after injecting it into the medium. Hence we diagnose the focusing by showing the time derivative  $\frac{\partial}{\partial t}(U_{total}(\hat{\mathbf{n}}', t) - U_{total}(\hat{\mathbf{n}}', -t))$ , injected into the medium.

Fig. 3(b) shows that for positive times, the wave field  $U_{total}(\hat{\mathbf{n}}', t) - U_{total}(\hat{\mathbf{n}}', -t)$  vanishes at the receivers for  $t < t_d(\hat{\mathbf{n}}')$ . If we consider this wave field at  $t = 0$ , the direct waves radiated at  $t = 0$  from  $\mathbf{x}_s$  arrive at a receiver location  $R(\hat{\mathbf{n}}')$  at  $t_d(\hat{\mathbf{n}}')$ . Suppose that waves would radiate at  $t = 0$  from a point  $\mathbf{x} \neq \mathbf{x}_s$ . For some receivers, those waves would arrive at a time  $t < t_d(\hat{\mathbf{n}}')$ ; however, as shown in Fig. 3(b), no waves arrive at time  $t < t_d(\hat{\mathbf{n}}')$ . This means that waves do not radiate from any point  $\mathbf{x} \neq \mathbf{x}_s$  at  $t = 0$ . Therefore, the time-derivative of the wave field  $U_{total}(\hat{\mathbf{n}}', t) - U_{total}(\hat{\mathbf{n}}', -t)$ , injected into the medium, is only non-zero at  $t = 0$  at the point  $\mathbf{x}_s$ , and the wave field focuses at  $t = 0$  at the virtual source location (see Appendix).

We let  $p(\mathbf{x}, t)$  denote the total wave field in the interior that is associated with the wave field  $U_{total}(\hat{\mathbf{n}}', t)$  on the boundary, and  $p(\mathbf{x}, -t)$  denote the time-reversed version of this wave field. The homogeneous Green's function ( $G_h(\mathbf{x}, \mathbf{x}_s, t) = G(\mathbf{x}, \mathbf{x}_s, t) - G(\mathbf{x}, \mathbf{x}_s, -t)$ ) (Oristaglio, 1989), for the virtual source location  $\mathbf{x}_s$  and the receiver location  $\mathbf{x}$  is, up to a multiplicative constant, obtained from (see also Appendix)

$$G_h(\mathbf{x}, \mathbf{x}_s, t) = p(\mathbf{x}, t) - p(\mathbf{x}, -t). \quad (7)$$

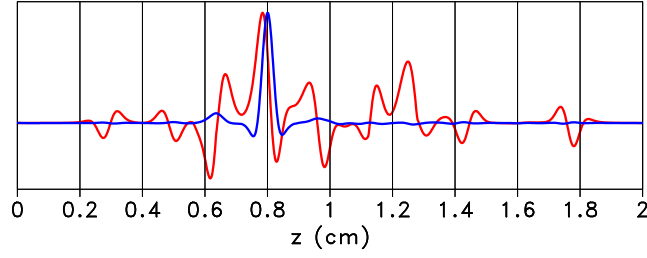


**Figure 4.** A normalized vertical cross-section of the snapshot at  $x = 4$  cm in Fig. 1(a) (red trace), and a normalized vertical cross-section of the snapshot at  $x = 4$  cm in Fig. 1(b) (blue trace). The blue trace is more concentrated at the focusing point at  $z = 0.8$  cm than the red trace.

If we want to focus a wave field at the virtual source location where there is no actual source located, we must have a non-zero incident wave field. The causal and acausal Green's functions satisfy the inhomogeneous acoustic wave equation, but the homogeneous Green's function  $G_h$  satisfies the homogeneous wave equation (Oristaglio, 1989). Eq. (7), therefore, retrieves the Green's function for  $t > 0$  for the virtual source location  $\mathbf{x}_s$ . Unlike other (interferometric) Green's function retrieval methods (Weaver and Lobkis, 2001; Campillo and Paul, 2003; Schuster, 2009; Snieder and Larose, 2013; Duroux et al., 2010; Roux et al., 2004; Sabra et al., 2005; Wapenaar et al., 2005), no physical receiver is required at the position of the virtual source; and unlike other Marchenko methods (Wapenaar et al., 2013, 2014), we do not rely on an up/down decomposition of the wave field. When one applies the Marchenko algorithm to two points in the interior, one obtains the Green's function for these two points recorded on the boundary. Using interferometric techniques, these Green's functions can be used to reconstruct the Green's function for waves propagating between two points in the interior (Singh and Snieder, 2017; Brackenhoff et al., 2019).

Fig. 3(c) shows the Green's function obtained from Eq. (7) with  $\mathbf{x}$  taken at the boundary (blue lines), superimposed on the directly-modeled Green's function (red lines). For clarity, the traces have been multiplied by  $\exp(2t)$  to emphasize the scattered waves. The latest arrival time for the single-scattered waves for our geometry is about  $18 \mu\text{s}$ . All waves arriving after  $18 \mu\text{s}$  therefore are multiply-scattered waves. For earlier times, the Green's function consists of a combination of single-scattered waves and multiply-scattered waves. As a result of our iterative solution, we retrieve the direct-wave and the scattered waves.

Fig. 4 shows normalized vertical cross-sections of the wave field at  $t = 0$  taken from Figs. 1(a) and 1(b) for  $x = 4$  cm. The red trace denotes the cross-section of Fig. 1(a) and the blue trace denotes the cross-section of Fig. 1(b). The snapshots (see Fig. 1) and the cross-sections (see Fig. 4) show that the reconstructed Green's function creates a focus only around the focusing point and cancels other arrivals around the focusing point to a large extent, whereas the results one can achieve with using only direct waves contain other arrivals that distort the focusing.

#### 4 CONCLUSION

We derive the 2D Marchenko equation for wave field focusing and Green's function retrieval for an arbitrary point in an unknown highly scattering inhomogeneous medium with a closed receiver array. We successfully retrieve the Green's function for a predefined location and the comparison to the directly-modeled Green's function is found to be excellent (see Fig. 3(c)). The cross-sections in Fig. 4 show that we can create better focusing in the medium than one can achieve with the direct waves only. Our retrieved Green's function contains both the single- and multiply-scattered waves of the heterogeneous medium model. Because we use a constant background velocity model, our method requires the direct-wave information modeled only in the homogeneous medium (when  $\rho$  is constant), and the recorded scattering response  $A(\hat{\mathbf{n}}, \hat{\mathbf{n}}', t)$  to solve the Marchenko equation iteratively like other multi-dimensional Marchenko methods proposed earlier (Wapenaar et al., 2013, 2014); however, it does not require wave field decomposition. We show that after the convergence, we retrieve the Green's function for any desired location in the medium without relying on prior information about the scatterers in the medium and wave field decomposition to solve the Marchenko equation. The Marchenko equation we propose forms the basis for imaging the interior of a medium inside a closed array without up/down decomposition and makes the Marchenko methods more appropriate for imaging steeply dipping structures.

## 5 ACKNOWLEDGMENTS

This work is supported by the Consortium Project on Seismic Inverse Methods for Complex Structures at the Colorado School of Mines. The numerical examples in this paper were generated using the Madagascar software package (<http://www.ahay.org>). The research of K. Wapenaar has received funding from the European Research Council (grant no. 742703).

## APPENDIX: THE HOMOGENEOUS GREEN'S FUNCTION RECONSTRUCTION

We provide a reasoning for Eq. (7) that is based on kinematic arguments, symmetry, and causality. In the following we assume that:

- (i) The wave field satisfies the wave equation for the real system.
- (ii) The reconstructed wave field is source free.
- (iii) The system is lossless and the wave field is invariant for time-reversal.
- (iv) The wave field is anti-symmetric in time.
- (v) For every point  $R\hat{\mathbf{n}}$  on the circle the wave field vanishes for  $-|R\hat{\mathbf{n}} - \mathbf{x}_f|/c < t < |R\hat{\mathbf{n}} - \mathbf{x}_f|/c$ .

In general, the wave field from sources  $f(\mathbf{x}_s, \tau)$  can be written as

$$\tilde{u}(\mathbf{x}, t) = \iiint G(\mathbf{x}, \mathbf{x}_s, t - \tau) f(\mathbf{x}_s, \tau) d\tau dV_s, \quad (\text{A-1})$$

where  $\tilde{u}(\mathbf{x}, t)$  denotes the wave field in the interior, and  $G(\mathbf{x}, \mathbf{x}_s, t)$  denotes the Green's function. Because the Green's function satisfies the wave equation for the real system, property (i) is satisfied for the wave field in expression (A-1). This expression specifies the wave field in terms of the sources  $f(\mathbf{x}_s, \tau)$ . It is, however, known that the inverse source problem is ill-posed (Bleistein and Cohen, 1977; Devaney and Sherman, 1982), hence for a given value of the wave field at the circle  $\mathbf{x} = R\hat{\mathbf{n}}$ , the source function  $f(\mathbf{x}_s, \tau)$  is not unique. We show, however, that properties (ii)-(v) constrain this function up to a multiplicative constant.

Because of the property (iv), the wave field is anti-symmetric in time and using the property (iii), solutions are invariant for time-reversal, we can create an anti-symmetric wave field by taking the difference of  $\tilde{u}(\mathbf{x}, t)$  and its time-reversed version  $\tilde{u}(\mathbf{x}, -t)$  as

$$u(\mathbf{x}, t) = \tilde{u}(\mathbf{x}, t) - \tilde{u}(\mathbf{x}, -t) = \iiint (G(\mathbf{x}, \mathbf{x}_s, t - \tau) f(\mathbf{x}_s, \tau) - G(\mathbf{x}, \mathbf{x}_s, -t - \tau) f(\mathbf{x}_s, \tau)) d\tau dV_s. \quad (\text{A-2})$$

By construction, this solution satisfies property (iv).

The Green's function satisfies

$$LG(\mathbf{x}, \mathbf{x}_s, t) = \delta(\mathbf{x} - \mathbf{x}_s)\delta(t), \quad (\text{A-3})$$

where  $L$  denotes the differential operator for the acoustic wave equation. Applying the operator  $L$  to the property (A-2) and carrying out the integrations over  $\tau$  and  $\mathbf{x}_s$  gives

$$Lu(\mathbf{x}, t) = f(\mathbf{x}, t) - f(\mathbf{x}, -t). \quad (\text{A-4})$$

The right hand side of this expression gives the sources of the wave field  $u(\mathbf{x}, t)$ . According to property (ii), the wave field is source-free, therefore, the right hand side of expression (A-4) vanishes, so that

$$f(\mathbf{x}, t) = f(\mathbf{x}, -t), \quad (\text{A-5})$$

showing that  $f(\mathbf{x}, t)$  is symmetric in time.

By using expression (A-5), we can replace the last term  $f(\mathbf{x}_s, \tau)$  in expression (A-2) by  $f(\mathbf{x}_s, -\tau)$ . Replacing next the integration variable  $\tau$  by  $-\tau$  in the second term reduces expression (A-2) to

$$u(\mathbf{x}, t) = \iiint (G(\mathbf{x}, \mathbf{x}_s, t - \tau) - G(\mathbf{x}, \mathbf{x}_s, \tau - t)) f(\mathbf{x}_s, \tau) d\tau dV_s. \quad (\text{A-6})$$

This expression can be written as

$$u(\mathbf{x}, t) = \iiint G_h(\mathbf{x}, \mathbf{x}_s, t - \tau) f(\mathbf{x}_s, \tau) d\tau dV_s, \quad (\text{A-7})$$

where  $G_h(\mathbf{x}, \mathbf{x}_s, t) = G(\mathbf{x}, \mathbf{x}_s, t) - G(\mathbf{x}, \mathbf{x}_s, -t)$  is the homogeneous Green's function defined in Eq. (7) in the main text. The homogeneous Green's function is source-free (Oristaglio, 1989), so it is natural that the homogeneous Green's function arises from the requirement that the wave field is source-free.

We next apply the property (v) to further constrain  $f(\mathbf{x}_s, \tau)$ . For positive times, the homogeneous Green's function  $G_h(\mathbf{x}, \mathbf{x}_s, t -$

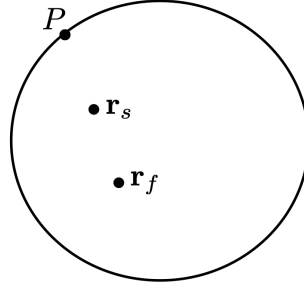


**Figure A-1.** Definition of the point  $P$  given locations  $\mathbf{x}_s$  and  $\mathbf{x}_f$ .

$\tau$ ) has a first arriving wave at location  $\mathbf{x}$  that is excited at  $\mathbf{x}_s$  and time  $\tau$  at time

$$t = \tau + |\mathbf{x} - \mathbf{x}_s|/c. \quad (\text{A-8})$$

According to expression (A-5), the function  $f(\mathbf{x}_s, \tau)$  is symmetric in time. This means that for every time source at  $\mathbf{x}_s$  at time  $\tau$ , there is an equal contribution from a source at  $\mathbf{x}_s$  at time  $-\tau$ , which generates a first arriving wave at

$$t = -\tau + |\mathbf{x} - \mathbf{x}_s|/c. \quad (\text{A-9})$$

The time  $\tau$  can be either positive or negative. Hence the first arriving wave arrives at  $t = \min(\tau, -\tau) + |\mathbf{x} - \mathbf{x}_s|/c$ . Since  $\min(\tau, -\tau) = -|\tau|$ , the first arrival excited by a source at  $\mathbf{x}_s$  at time  $\pm\tau$  arrives at the point  $\mathbf{x}$  at time

$$t = -|\tau| + |\mathbf{x} - \mathbf{x}_s|/c. \quad (\text{A-10})$$

For a point  $R\hat{\mathbf{n}}$  on the circle, the first arriving wave excited at a point  $\mathbf{x}_s$  at time  $\pm\tau$  arrives at

$$t = -|\tau| + |R\hat{\mathbf{n}} - \mathbf{x}_s|/c. \quad (\text{A-11})$$

Property (v) states that for positive time  $t$  and a point  $R\hat{\mathbf{n}}$  on the circle, the wave field vanishes when

$$t < |R\hat{\mathbf{n}} - \mathbf{x}_f|/c, \quad (\text{A-12})$$

where  $\mathbf{x}_f$  is the focusing point. Since the wave field vanishes for these times, the first arriving waves that are excited at  $\mathbf{x}_s$  must have an arrival times greater or equal to  $|R\hat{\mathbf{n}} - \mathbf{x}_f|/c$ . Using expression (A-11), this implies that

$$-|\tau| + |R\hat{\mathbf{n}} - \mathbf{x}_s|/c \geq |R\hat{\mathbf{n}} - \mathbf{x}_f|/c, \quad (\text{A-13})$$

We can also write this inequality as

$$c|\tau| \leq |R\hat{\mathbf{n}} - \mathbf{x}_s| - |R\hat{\mathbf{n}} - \mathbf{x}_f|, \quad (\text{A-14})$$

Note that the focusing point  $\mathbf{x}_f$  is specified, while the point  $\mathbf{x}_s$  can be anywhere within the circle of radius  $R$ .

Let us consider a point  $\mathbf{x}_s \neq \mathbf{x}_f$ , as shown in Fig. A-1. For the point  $P$  in that figure  $|R\hat{\mathbf{n}} - \mathbf{x}_s| < |R\hat{\mathbf{n}} - \mathbf{x}_f|$ , the inequality (A-14) reduces to  $c|\tau| \leq |R\hat{\mathbf{n}} - \mathbf{x}_s| - |R\hat{\mathbf{n}} - \mathbf{x}_f| < 0$ , or  $c|\tau| < 0$ . This inequality cannot be satisfied for any value of  $\tau$ , which means that a point  $\mathbf{x}_s \neq \mathbf{x}_f$  cannot be a source of the wave field.

Consider next the case  $\mathbf{x}_s = \mathbf{x}_f$ . In that case the inequality (A-14) reduces to  $c|\tau| \leq 0$ . This inequality can only be satisfied for  $\tau = 0$ . Together with the fact that  $f(\mathbf{x}_s, \tau)$  is only nonzero for  $\mathbf{x}_s = \mathbf{x}_f$ , this implies that the source-time function is local in space and time

$$f(\mathbf{x}_s, \tau) = S\delta(\mathbf{x}_s - \mathbf{x}_f)\delta(\tau), \quad (\text{A-15})$$

where  $S$  is a multiplicative constant. Note that any even time derivative of  $\delta(t)$  would also give the required localization in time. Since in any physical experiment and computer simulation the wave field is convolved with a wavelet, we ignore this subtlety.

Inserting this source function into expression (A-7), and carrying out the integration over  $\mathbf{x}_s$  and  $\tau$  gives

$$u(\mathbf{x}, t) = SG_h(\mathbf{x}, \mathbf{x}_f, t). \quad (\text{A-16})$$

This implies that, up to a multiplicative constant  $S$ , the wave field is given by the homogeneous Green's function with a source at the focusing point.

## REFERENCES

- Bleistein, N., and J. Cohen, 1977, Nonuniqueness in the inverse source problem in acoustics and electromagnetics: *J. Math. Phys.*, **18**, 194–201.
- Brackenhoff, J., J. Thorbecke, and K. Wapenaar, 2019, Virtual sources and receivers in the real earth: Considerations for practical applications: *Journal of Geophysical Research: Solid Earth*, **124**, 11802–11821.
- Broggini, F., and R. Snieder, 2012, Connection of scattering principles: a visual and mathematical tour: *European Journal of Physics*, **33**, 593–613.
- Burridge, R., 1980, The Gelfand-Levitan, the Marchenko, and the Gopinath-Sondhi integral equations of inverse scattering theory, regarded in the context of inverse impulse-response problems: *Wave Motion*, **2**, 305–323.
- Campillo, M., and A. Paul, 2003, Long-range correlations in the diffuse seismic coda: *Science*, **299**, 547–549.
- Chadan, K., and P. C. Sabatier, 1989, *Inverse problems in quantum scattering theory*: Springer.
- Colton, D., and R. Kress, 1998, *Inverse acoustic and electromagnetic scattering theory*: Springer.
- Devaney, A., and G. Sherman, 1982, Nonuniqueness in inverse source and scattering problems: *IEEE Trans. on Antennas and Propagation*, **AP-30**, 1034–1037.
- Diekmann, L., and I. Vasconcelos, 2021, Focusing and Green’s function retrieval in three-dimensional inverse scattering revisited: A single-sided Marchenko integral for the full wave field: *Phys. Rev. Research*, **3**, no. 1, 013206.
- Duroux, A., K. Sabra, J. Ayers, and M. Ruzzene, 2010, Using cross-correlations of elastic diffuse fields for attenuation tomography of structural damage: *J. Acoust. Soc. Am.*, **127**, 3311–3314.
- Gladwell, G. M. L., 1993, *Inverse problems in scattering*: Kluwer Academic Publishing.
- Kiraz, M. S. R., R. Snieder, and K. Wapenaar, 2020, Marchenko focusing without up/down decomposition: *SEG Technical Program Expanded Abstracts 2020*, 3593–3597.
- Newton, R. G., 1980a, Inverse scattering. I. one dimension: *Journal of Mathematical Physics*, **21**, 493–505.
- , 1980b, Inverse scattering. II. three dimensions: *Journal of Mathematical Physics*, **21**, 1698–1715.
- , 1981, Inverse scattering. III. three dimensions, continued: *Journal of Mathematical Physics*, **22**, 2191–2200.
- , 1982, Inverse scattering. IV. three dimensions: generalized Marchenko construction with bound states, and generalized Gel’fand–Levitan equations: *Journal of Mathematical Physics*, **23**, 594–604.
- Oristaglio, M. L., 1989, An inverse scattering formula that uses all the data: *Inverse Problems*, **5**, 1097–1105.
- Ricker, N., 1953, Wavelet contraction, wavelet expansion, and the control of seismic resolution: *GEOPHYSICS*, **18**, 769–792.
- Rose, J. H., 2001, ‘Single-sided’ focusing of the time-dependent Schrödinger equation: *Phys. Rev. A*, **65**, no. 1, 012707.
- , 2002, ‘Single-sided’ autofocusing of sound in layered materials: *Inverse Problems*, **18**, 1923–1934.
- Roux, P., W. Kuperman, and N. Group, 2004, Extracting coherent wave fronts from acoustic ambient noise in the ocean: *J. Acoust. Soc. Am.*, **116**, 1995–2003.
- Sabra, K., P. Gerstoft, P. Roux, W. Kuperman, and M. Fehler, 2005, Extracting time-domain Green’s function estimates from ambient seismic noise: *Geophys. Res. Lett.*, **32**, L03310.
- Schuster, G. T., 2009, *Seismic interferometry*: Cambridge University Press.
- Singh, S., and R. Snieder, 2017, Strategies for imaging with Marchenko-retrieved Green’s functions: *GEOPHYSICS*, **82**, Q23–Q37.
- Snieder, R., and E. Larose, 2013, Extracting earth’s elastic wave response from noise measurements: *Annual Review of Earth and Planetary Sciences*, **41**, 183–206.
- Wapenaar, K., F. Broggin, E. Slob, and R. Snieder, 2013, Three-dimensional single-sided Marchenko inverse scattering, data-driven focusing, Green’s function retrieval, and their mutual relations: *Phys. Rev. Lett.*, **110**, no. 8, 084301.
- Wapenaar, K., F. Broggin, and R. Snieder, 2012, Creating a virtual source inside a medium from reflection data: heuristic derivation and stationary-phase analysis: *Geophysical Journal International*, **190**, 1020–1024.
- Wapenaar, K., J. Fokkema, and R. Snieder, 2005, Retrieving the Green’s function by cross-correlation: a comparison of approaches: *J. Acoust. Soc. Am.*, **118**, 2783–2786.
- Wapenaar, K., R. Snieder, S. de Ridder, and E. Slob, 2021, Green’s function representations for Marchenko imaging without up/down decomposition: *arXiv:2103.07734*.
- Wapenaar, K., J. Thorbecke, J. van der Neut, F. Broggin, E. Slob, and R. Snieder, 2014, Marchenko imaging: *GEOPHYSICS*, **79**, WA39–WA57.
- Weaver, R. L., and O. I. Lobkis, 2001, Ultrasonics without a source: Thermal fluctuation correlations at mhz frequencies: *Phys. Rev. Lett.*, **87**, no. 13, 134301.